https://doi.org/10.15407/ujpe68.9.628

V.P. KOSTYLYOV, A.V. SACHENKO, T.V. SLUSAR, V.V. CHERNENKO

V. Lashkaryov Institute of Semiconductor Physics, Nat. Acad. of Sci. of Ukraine
(45, Nauky Ave., Kyiv 03028, Ukraine; e-mail: vkostylyov@ukr.net)

REDUCTION OF RECOMBINATION LOSSES IN NEAR-SURFACE DIFFUSION EMITTER LAYERS OF PHOTOSENSITIVE SILICON n^+-p-p^+ STRUCTURES

When creating an n^+-emitter in photosensitive structures of the n^+-p-p^+ type, the structure of its near-surface layer after the diffusion operation is found to be substantially damaged with increased recombination losses. The influence of additional growing-etching cycles of the silicon dioxide layer on the emitter surface when manufacturing such photosensitive silicon structures on their photoelectric and recombination characteristics is studied. It is shown that the application of such an additional treatment in the production of photosensitive silicon structures allows the recombination losses to be effectively reduced and, thereby, the photovoltaic parameters of such structures, including their spectral and threshold photosensitivities, to be significantly improved.

Keywords: photosensitive silicon structure, near-surface layer, emitter, recombination losses, heat treatments, silicon dioxide layer.

1. Introduction

Improving the characteristics of semiconductor photosensitive structures, in particular, silicon-based ones, which serve as a basis for the creation of such photosensitive devices as solar cells, photodiodes, photosensors, coordinate-sensitive elements, and others remains a challenging task for a long time [1–3]. This goal can be achieved in three ways: (i) by reducing the recombination losses of photogenerated non-equilibrium charge carriers in the emitter and base regions of the photosensitive silicon structure (PSS), (ii) by reducing optical losses via the reflection of light from the PSS photoreceptive surface, and (iii) by reducing ohmic losses induced by the negative effect of the insufficiently small series resistance and the insufficiently large shunt one of the PSS.

To reduce recombination losses, it is necessary to minimize the rate of recombination processes on the front and rear surfaces of the photosensitive structure, as well as in the bulk of its emitter and base regions. In this case, a reduction of recombination losses in the PSS base region and a decrease of the surface recombination rate at the PSS rare surface will increase the long-wave sensitivity of this structure. At the same time, a reduction of recombination losses in the heavily doped emitter region (the Auger recombination) and a decrease of the surface recombination rate at the front surface of the PSS will increase its short-wave sensitivity. It should be noted that a low level of recombination losses must also be provided in an already manufactured photosensitive device, because silicon undergoes various active physical and chemical treatments during the manufacture of a photosensitive structures, and those treatments can change the recombination characteristics of manufactured structures [4–9].

When fabricating PSSs with a classical design (the base is of the p-type, the thin heavily doped emitter region is formed near the photoreceiving surface of the device, and the base region with a moderate doping level and the opposite conductivity type is located between the emitter region and the heavily doped antirecombination p^+-layer and the rear contact), the

Citation: Kostylyov V.P., Sachenko A.V., Slusar T.V., Chernenko V.V. Reduction of recombination losses in near-surface diffusion emitter layers of photosensitive silicon n^+-p-p^+ structures. *Ukr. J. Phys.* **68**, No. 9, 628 (2023). https://doi.org/10.15407/ujpe68.9.628.

Цитування: Костильов В.П., Саченко А.В., Слусар Т.В., Черненко В.В. Зменшення рекомбінаційних втрат у дифузійних приповерхневих емітерних шарах фоточутливих кремнієвих структур n^+-p-p^+. *Укр. фіз. журн.* **68**, №9, 630 (2023).

initial stages of the surface oxidation of the highly doped emitter n^+-layer in such device, which was created via the thermal diffusion of phosphorus, were found to proceed much faster in comparison with the typical oxidation rates of the surface of moderately doped single-crystalline silicon. Additional studies of the surface morphology of the emitter n^+-region using the raster electron microscopy method showed that it has a highly defective, loose, and pore-like structure. It was suggested that such structural damage may be a result of the enhanced recombination losses in the PSS emitter region, which negatively affects its photoelectric parameters, in particular, the threshold sensitivity and the photosensitivity in the short-wavelength spectral region, the short-circuit current, and the open-circuit voltage. On the other hand, it is known that heat treatment operations are widely and successfully used to create Si–SiO_2 systems with good microstructural and electrophysical properties of the Si–SiO_2 interface [10–14].

The aim of this work is to study, in detail, the mechanisms of recombination losses in photosensitive n^+-p-p^+ silicon structures and search for ways to improve their photoelectric parameters and spectral sensitivity. We will try to decrease the recombination losses associated with the Auger recombination in their emitter layer (by optimizing the doping level of the latter) and to reduce the surface recombination (via passivating the front surface by means of a silicon dioxide layer with a built-in positive charge and creating the Si–SiO_2 interface with higher-quality microstructural and electrophysical properties).

2. Experimental Specimens and Methods

Experimental studies were carried out on PSS specimens with combined diffusion-field barriers [15]. Diffusion-field barriers are created both with the help of the thermal diffusion of shallow doping impurities and owing to the built-in positive charge N_{S0} of the silicon dioxide layer deposited onto the surface of the n^+-diffusion emitter layer (see Fig. 1, *a*). The application of photosensitive silicon-based structures with combined diffusion-field (induced) barriers makes it possible to combine the advantages of the diffusion and inversion PSSs and get rid of their disadvantages [15–17].

The presence of a strong electric field (10^5–10^6 V/cm) in PSSs with induced barriers and a small depth of the induced junction location (≤ 0.1 μm) lead to the situation, when practically all electron-hole pairs generated by electromagnetic (light) irradiation in the near-surface region of silicon are brought apart without recombination by the field, so that they can contribute to the photocurrent. As a result, two positive effects take place [15–17]. First, even a relatively high concentration of electronic states at the dielectric-semiconductor interface weakly affects the surface recombination rate at the illuminated PSS surface and the photocurrent magnitude. Second, the short-wavelength photosensitivity in PSSs with induced barriers turns out much higher than in ordinary diffusion PSSs, which allows the former to be used, in particular, in ultraviolet radiation detectors.

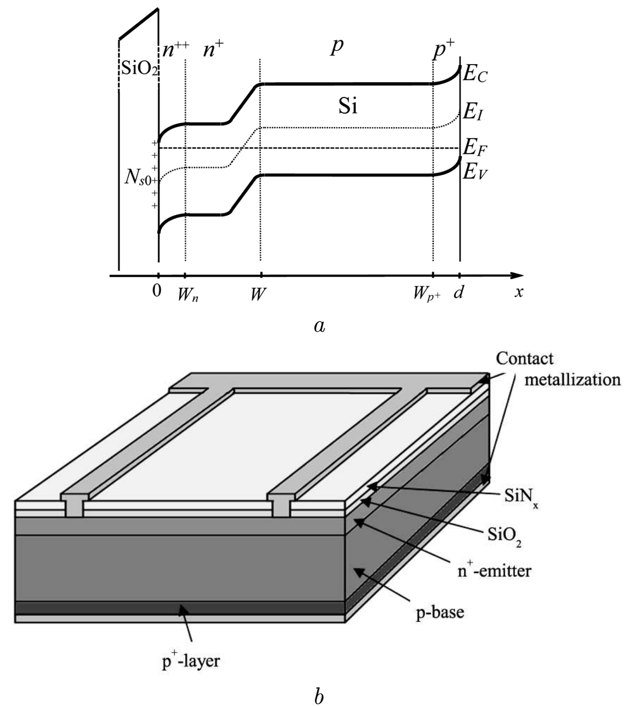

Fig. 1. Band diagram (*a*) and schematic diagram (*b*) of a photosensitive silicon structure with combined diffusion-field barriers

The experimental PSS specimens were fabricated on the basis of KDB-9 silicon plates with the p-type conductivity, the specific resistance $\rho \approx 9$ Ω cm (the concentration of the doping acceptor impurity $N_a = 1.51 \times 10^{15}$ cm^{-3}), a thickness of 380 μm, and an area of 5×5 mm^2. The n^+-type emitter was formed by the thermal diffusion of phosphorus for 26 min at the temperature $T = 940$ °C. For the pas-

sivation of the specimen and the reduction of optical losses, a two-layer anti-reflective $SiO_2 + Si_3N_4$ coating was deposited onto the front (illuminated) surface of the specimens. To reduce the recombination at the metal-silicon contact, an anti-recombination p-p^+ junction [15] was formed on the rear specimen surface by the thermal diffusion of boron for 20 min at $T = 985$ °C. Afterward, a continuous aluminum contact was deposited onto it. An aluminum contact in the form of a grid of narrow "fingers" connected to a wider busbar was created on the photo-receptive front surface (Fig. 1, *b*). The shaded area of the front surface did not exceed 7%.

In order to study whether it is possible to improve the characteristics of examined photosensitive structures by reducing the recombination losses in their emitter n^+-region, the frontal photoreceptive surfaces of the emitter layer of the specimens belonging to different experimental groups, but manufactured in the same technological process were subjected to additional (from one to three) treatment cycles (the etching and growing of the oxide layer), which was aimed at transforming the thin near-surface porous silicon layer into a silicon dioxide one and then removing the latter by the subsequent etching. The SiO_2 layer was grown in the chlorine environment (in HCl vapors) for 40 min at a temperature of 1050 °C and then etched off in the hydrofluoric acid. Afterward, the specimens were thoroughly washed in deionized water. The thickness of the thermally grown SiO_2 layer before its etching was 110 ± 10 nm. After the manufacturing process was completed, the following studies were performed for various experimental groups of PSS specimens:

• the measurements of the light current-voltage characteristics (CVCs) under standard AM0 conditions (the energy illuminance $P_L = 1360$ W/m^2, the temperature $T = 25$ °C); the results were used to determine the main photoelectric and recombination parameters;

• the measurements of the spectral dependences of the short-circuit current under the automatic maintenance of a constant energy illuminance level in a wavelength interval of 400–1200 nm; the results were used to determine the spectral dependences of the external quantum efficiency;

• the measurements of the dark CVCs; the results were used to determine the dark reverse current values at applied voltages of 0.01, 1, and 5 V.

The obtained results were compared with analogous characteristics and parameters obtained for the PSS specimens in the control group. The latter were manufactured in the same technological process, but without the mentioned additional growing-etching cycles of the oxide layer on their photoreceptive surfaces. Every experimental group included 8–10 specimens.

The analysis of the light CVCs makes it possible, in particular, to study the behavior of the short-circuit current in photosensitive structures. Its value is determined by the collection efficiency of photogenerated charge carriers. By analyzing the spectral dependences of the short-circuit current, it is possible to determine the peculiarities in the evolution of recombination processes, which, in turn, affect the collection efficiency of non-equilibrium charge carriers in those photosensitive structures. The determination of the values of the reverse dark currents at various applied voltages also allows a comparative study of the levels of recombination losses in manufactured specimens belonging to different groups. Furthermore, the lower the values of the dark currents, the higher the threshold sensitivity, which is an extremely important characteristic for photosensitive structures intended for the manufacture of photosensors.

It should be added that the measurements of light CVCs and spectral dependences were carried out on a metrologically certified bench base, namely, on an installation for phototechnical tests of solar cells and an installation for determining the relative spectral characteristics of photoconverters, respectively, at the Center for testing photo-conversion devices and photovoltaic arrays of the V. Lashkaryov Institute of Semiconductor Physics of the National Academy of Sciences of Ukraine, which was certified by the State authorities of Ukraine for technical competence and independence [18, 19].

3. Experimental Results and Their Discussion

The results of experimental studies demonstrate that additional heat treatments brought about a substantial decrease of the rate of emitter surface oxidation followed by its stabilization. This fact testifies to the removal of the pore-like structurally imperfect near-surface layer in the course of the diffusional creation of the emitter.

The light CVCs were measured for experimental PSS specimens in all groups. The specimens in the control group (group 0) were not subjected to the additional heat treatments and the removal of the oxide layer that was formed on the emitter n^+-layer when those specimens were produced. The specimens in groups 1 to 3 underwent an additional heat treatment in the form of the cycles of the etching and thermal growth of the SiO_2 layer on their front surfaces. The group numbers correspond to the number of additional growing-etching cycles. The obtained light CVCs were used to determine the photovoltaic parameters and the effective lifetime of non-equilibrium minor charge carriers in the manufactured experimental PSS specimens belonging to various groups.

In order to determine the lifetime of non-equilibrium electrons, we used an approach that was developed and described in detail in works [20–22]. Here, we describe it in a somewhat simplified form. Using the generation-recombination balance equation for an open PSS circuit in the approximation that light absorption is uniform over the specimen thickness, we obtain

$$R = \frac{\Delta n_{\rm oc}}{\tau_{\rm eff}} = G = \frac{J_{\rm sc}}{qd}, \qquad (1)$$

$$\frac{1}{\tau_{\rm eff}} = \frac{1}{\tau_b} + \frac{1}{\tau_A} + \frac{S_\Sigma}{d}, \qquad (2)$$

$$J_{\rm sc} = q\frac{d}{\tau_{\rm eff}}\Delta n_{\rm oc}, \qquad (3)$$

where $J_{\rm sc}$ is the short-circuit current density, q the elementary charge, d the thickness of the PSS base region, $\tau_{\rm eff}$ the effective lifetime of non-equilibrium electron-hole pairs, τ_b the bulk lifetime, τ_A the lifetime before the recombination according to the Auger mechanism, S_Σ the sum of surface recombination rates at both surfaces, and $\Delta n_{\rm oc}$ the excess concentration of electron-hole pairs under open-circuit conditions. The latter parameter is given by the equation [20–22]

$$\Delta n_{\rm oc} = -\frac{n_0}{2} + \sqrt{\frac{n_0^2}{4} + n_i^2 \exp\left(\frac{V_{\rm oc}}{kT}\right)}, \qquad (4)$$

where n_0 is the equilibrium concentration of electron-hole pairs (for the studied PSS specimens, it is determined by their doping levels), $V_{\rm oc}$ the open-circuit voltage, and n_i the intrinsic concentration of electron-hole pairs in silicon. The temperature dependence of n_i is given by the expression [23]

$$n_i\,(T) = 2.9135 \times 10^{15}\; T^{1.6} \exp\left(-\frac{E_g\,(T)}{kT}\right), \qquad (5)$$

where

$$E_g(T) = 1.17 + 2.143 \times 10^{-5}\; T - 7.85 \times 10^{-7}\; T^2 + \\ + 6.835 \times 10^{-10}\; T^3 \qquad (6)$$

is the temperature dependence of the band gap width in silicon [24].

Note that the band-narrowing effect [20] is not taken into account in Eq. (4). This approximation is valid, if the $\Delta n_{\rm oc}$-values are not very high ($\Delta n_{\rm oc} \lesssim$ $\lesssim 10^{15}$ cm^{-3}).

From Eq. (3), we obtain the following dependence of the effective lifetime on the excitation (injection) level:

$$\tau_{\rm eff}(\Delta n_{\rm oc}) = \frac{qd\Delta n_{\rm oc}}{J_{\rm sc}}. \qquad (7)$$

In our case, the effective lifetime of non-equilibrium electron-hole pairs in PSSs is mainly determined by the bulk recombination, the interband and exciton Auger recombination, and the surface recombination [25, 26],

$$\tau_{\rm eff} \approx \left(\frac{1}{\tau_b} + \frac{1}{\tau_A} + \frac{S_0}{d}\right)^{-1}, \qquad (8)$$

where S_0 is the surface recombination rate at the front surface. It should be noted that only such parameters as τ_A and S_0 change owing to the growing-etching processes of the oxide layer on the front surface.

The values of the photoelectric and recombination parameters determined for the fabricated experimental PSS specimens from various groups are shown in Table 1. As one can see from the presented results, the values of the short-circuit current in the specimens of group 1 (after one growing-etching cycle of the oxide layer on the front surface of the photosensitive structures) increased by approximately 10% in comparison with the specimens of the control group 0 (from 5.7–5.8 to 6.3–6.4 mA), and the values of the open-circuit voltage by about 3% (from 590–595 to 605–615 mV). The effective lifetime of minor charge carriers also increased, which testifies to a positive effect of the additional heat treatment and is a consequence of a substantial reduction of the recombination rates at the surface and in the near-surface layer of the emitter region. The application of two

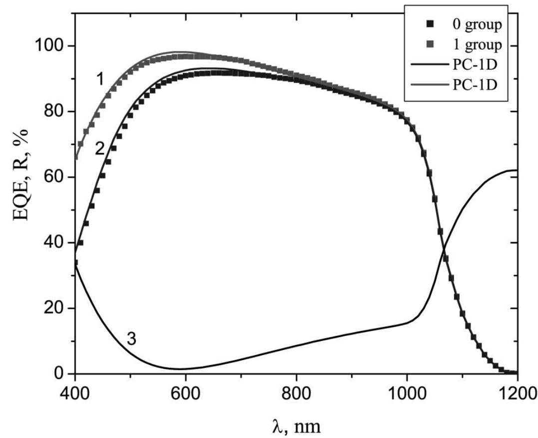

Fig. 2. Typical spectral dependences of the external quantum efficiency *EQE* obtained for the experimental specimens of photosensitive structures from control group 0 (squares) and group 1 (triangles). Curves *1* and *2* show the simulation results obtained for experimental spectra using the PC-1D program. Curve *3* is the spectral dependence of the reflection coefficient for the SiN_x–SiO_2 system calculated taking multiple reflections in the specimen into account

Table 1. **Influence of the number of additional growing-etching cycles of the SiO_2 layer on photoelectric and recombination parameters of experimental PSS specimens**

Group	Number of additional heat treatments	Short-circuit current I_{sc}, mA	Open-circuit voltage V_{oc}, mV	Effective lifetime τ_{eff}, μs
0	0	5.7–5.8	590–595	99–100
1	1	6.3–6.4	605–615	160–162
2	2	5.1–5.9	575–600	64–111
3	3	5.7–6.4	595–610	104–157

and three cycles of the oxide layer growing-etching does not increase further the values of photovoltaic parameters and effective lifetime in comparison with those for the specimens of group 1. On the contrary, some deterioration of the photovoltaic parameters is observed, which, as is known, may be associated with the formation of recombination centers in the bulk, if the total time of high-temperature treatments during the oxidation process is long (see, for example, works [27, 28]).

The analysis of the results obtained for the spectral dependences of the external quantum efficiency, *EQE*, showed that the value of the spectral photosensitivity in a wavelength interval of 400–800 nm increased considerably for the experimental specimens in group 1 (they were fabricated using one cycle of the oxide layer growing-etching on their front surfaces) in comparison with the corresponding value obtained for the experimental specimens in control group 0 (they were fabricated with no additional growing-etching cycles of the SiO_2 layer, Fig. 2). In particular, the value of spectral photosensitivity became approximately twice as large at a wavelength of 400 nm. Such a photosensitivity growth is connected with a decrease of recombination losses in the emitter due to the removal of its near-surface porous layer via the additional operation of the oxide layer growing and etching. Additional (two or three) growing-etching cycles lead to a certain photosensitivity reduction in a wavelength interval of 400–800 nm for the experimental specimens in groups 2 and 3 in comparison with that for the specimens in group 1, which may also be associated with the formation of bulk recombination centers, if the total time of high-temperature treatments is long. Nevertheless, the specimens in groups 2 and 3 had a much higher photosensitivity in a wavelength interval of 400–800 nm as compared with the specimens in control group 0; in particular, the photosensitivity value at a wavelength of 400 nm for the specimens in groups 2 and 3 was 1.5–1.8 times higher in comparison with that for the specimens in the control group.

The experimental spectral dependences of the external quantum efficiency *EQE* for the PSS specimens in groups 0 (control) and 1 were simulated using the PC-1D software program [29]. The simulation results are shown in Fig. 2 (curves *1* and *2*). One can see a good agreement between the experimental and theoretical dependences. The parameters of theoretical curves are quoted in Table 2.

From the analysis of the data in Table 2, it follows that even if one additional growth-etching cycle for the SiO_2 layer is performed, the surface recombination rate at the front surface decreases by two orders of magnitude, and the maximum surface concentration of major carriers decreases by a factor of five, to 3×10^{19} cm^{-3}. The resistance of the emitter layer becomes approximately 3 times lower at that. The decrease in the surface concentration of major carriers leads to a substantial decrease of the Auger recombination rate in the emitter layer. Hence, the reduction of the surface and Auger recombination rates gives rise to the growth of the effective lifetime in the PSS in accordance with Eq. (8).

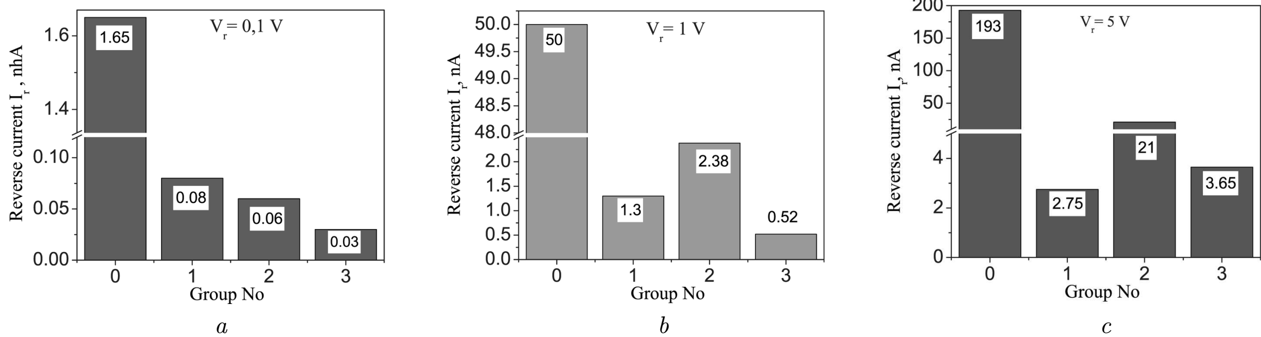

Fig. 3. The influence of the number of additional growing-etching cycles of the SiO_2 layer on the average value of reverse dark currents I_r in experimental PSS specimens for various values of the applied reverse voltage $V_r = 0.01$ (*a*), 1 (*b*), and 5 V (*c*)

It was already mentioned that the determination of the reverse dark current values at various applied voltages makes it possible to carry out a comparative study of the recombination loss levels in the emitter layers of the manufactured PSS specimens from different groups and, accordingly, their threshold sensitivities. The distributions of the reverse dark current values over the groups of the examined experimental specimens at various applied voltages (0.01, 1, and 5 V) are shown in Fig. 3.

The dependences of the reverse current on the applied voltage ($I_r(V_r)$, the reverse branch of the dark CVC) are shown in Fig. 4. The plots are exhibited on the log-log scale in order to demonstrate the total range of the reverse current variation, because the specimens from control group 0 had reverse currents by orders of magnitude larger than the specimens from other groups. If the same dependences are plotted on the linear scale along both axes, their character can be determined. In particular, the dependences $I_r(V_r)$ for the specimens from groups 0 and 1 have a sublinear character and the increasing values of the equivalent shunt resistance, as the reverse voltage increases; the dependences for the specimens from group 2 have a superlinear character and the decreasing values of the equivalent shunt resistance. Finally, the dependences for the specimens from group 3 have a character close to linear (see Table 3). Those specific features can be used to select the optimal mode for the operation of such structures with the reverse bias.

From the analysis of the data depicted in Figs. 3 and 4, one can see that the values of the reverse dark currents for the experimental PSS specimens in group 1 are lower by more than an order of magnitude

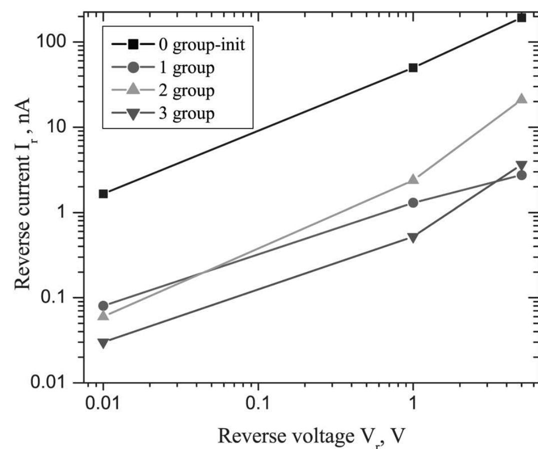

Fig. 4. Reverse branches of the dark CVCs for PSS specimens subjected to various numbers of growing-etching treatment cycles of the SiO_2 layer and without etching the SiO_2 layer (initial control group 0, squares)

Table 2. **Parameters of theoretical spectral dependences of *EQE* (Fig. 2)**

Parameter	Curve *1*	Curve *2*
Base thickness, μm	380	380
Base doping level, cm^{-3}	1.5×10^{15}	1.5×10^{15}
Lifetime in the base, s	1.6×10^{-4}	1.6×10^{-4}
Emitter doping		
profile	Erfc	Erfc
peak level, cm^{-3}	3×10^{19}	1.5×10^{20}
layer resistance, $\Omega/\square$	90	26
Surface recombination rate, cm/s		
front surface	10^3	10^5
rare surface	10^3	10^3
SiO_2 layer thickness, nm	30	30
Si_3N_4 layer thickness, nm	45	45

in comparison with the values obtained for the experimental PSS specimens in control group 0. A larger number of the growing-etching cycles for the oxide layer on the emitter surface (not at all applied voltage values) leads to a further reduction of the reverse dark current values. However, it should be noted that, after three growing-etching cycles, the reverse dark currents in the experimental PSS specimens (group 3) were almost two orders of magnitude lower in comparison with the values obtained for the specimens from the control group.

To explain the obtained results, let us apply the analysis of the data presented in works [30, 31]. In []30], the "self-gettering" effect was revealed which occurred, when the active emitter n^+-regions were formed in p-type silicon using the thermal diffusion of phosphorus. Namely, the volume of the silicon substrate became, to a great extent, cleared of generation-recombination complexes, which manifested itself in the growth of the diffusion path length of minor charge carriers, the homogenization of the recombination characteristics of the space charge region, as well as the diminishing of the reverse currents to the current saturation level of the reverse-biased n^+-p-junction typical of a defect-free material, simultaneously with the deterioration of the recombination parameters of the n^+-region owing to its contamination with impurities and defects gettered from the bulk and rapidly diffusing. Just the features indicated above were observed in the photovoltaic parameters of the studied structures, when thermally growing silicon oxide, first of all for the structures of groupe 1. In work [31], it was also proved that, when creating n^+-p-junctions in p-type silicon plates in the standard diffusion modes used in industry, the effect of recombination-impurity gettering takes place, and the effective lifetime of non-equilibrium charge carriers in the bulk grows.

Table 3. **Influence of the number of additional growing-etching cycles of the SiO_2 layer on the equivalent shunt resistance of experimental PSS specimens**

Group	Reverse voltage, V		
	0.01	1	5
	Equivalent shunt resistance, Ω		
0	6.06×10^6	2.00×10^7	2.59×10^7
1	1.25×10^8	7.69×10^8	1.82×10^9
2	1.67×10^8	4.20×10^8	2.38×10^8
3	3.33×10^8	1.92×10^9	1.37×10^9

Thus, in our case, during the primary formation of the emitter n^+-region in the experimental PSS specimens of all groups, the "self-gettering" effect [30] takes place, i.e., the volume of the silicon wafer becomes cleared from recombination impurities and defects, which are removed into the heavily doped n^+-region because of the increased solubility of metal impurities in phosphorus-doped silicon [32, 33]. Therefore, as a result of the concentration growth of the recombination centers in the n^+-region, the surface recombination rate increases, and the photosensitivity decreases in the short-wavelength spectral region at the wavelengths $\lambda < 600$ nm. The volume of the silicon substrate becomes, to a great extent, cleared of rapidly diffusing impurities and defects, which is manifested in the longer lifetime of minor charge carriers in the base p-region of experimental PSS specimens. The further heat treatment of the specimens (for 10 min in the case of the specimens from group 0 and 40 min in the case of the specimens from groups 1, 2, and 3) at a temperature of 1050 °C during their oxidation in HCl vapors favors the additional gettering and the effect enhancement. As a result, the gettered recombination impurities and defects in the specimens of groups 1, 2, and 3 transit into the grown silicon oxide layer with a thickness of 110 ± 10 nm. The subsequent etching of this oxide layer fulfils two task: a) it removes recombination impurities and defects, and b) it controllably reduces the thickness of the heavily doped n^+-region, thus reducing the negative effect of the interband and exciton Auger recombination [15]. Analogous processes take place during the further oxidation-etching cycles.

The simulation results for the spectral dependences of the external quantum efficiency, which were obtained using the PC-1D program and described earlier, confirm the proposed model representation of the processes occurring in the researched PSS specimens.

Additional oxidation-etching treatments of the specimens in groups 1, 2, and 3 prolong the effective lifetime (Table 1). It occurs, first of all, owing to the reduction of the recombination rate at the surface and in the emitter [Eq. (8)]. As a result, a substantial increase of the short-wavelength photosensitivity (Fig. 2), a growth of the short-circuit current and open-circuit voltage, and a decrease of the reverse

current values within the whole interval of applied reverse voltages (Figs. 3 and 4) take place, i.e., all main characteristics of PSSs become better.

As one can see from the presented data, the most pronounced improvement of the parameters of the researched PSS specimens was attained after the first additional oxidation-etching treatment, which testifies that the initial silicon was rather pure and with a low concentration of recombination impurities and defects. This conclusion is also evidenced by rather large lifetime values for non-equilibrium minor charge carriers in the specimens of group 0.

To summarize, note that the application of one to three cycles of the oxide layer growing-etching on the emitter surface with combined diffusion-field (induced) barriers considerably diminishes the level of recombination losses in the examined specimens, increases the short-wave spectral photosensitivity, and significantly improves the threshold photosensitivity of PSSs.

4. Conclusions

As a result of the research carried out in this work, it is found that the surface of a heavily doped emitter layer created by the diffusion contains a thin near-surface damaged region with a porous structure. This region induces considerable recombination losses in photosensitive silicon structures, which are responsible for a strong reduction of the values of the short-circuit current, the open-circuit voltage, the effective lifetime of non-equilibrium current carriers, and the photosensitivity in the short-wave spectral interval at wavelengths of 400–800 nm. A high level of recombination losses is confirmed by appreciable values of reverse dark currents and is the origin of a low threshold sensitivity of such structures.

It was experimentally shown that the additional heat treatment of the specimens in the HCl environment, which includes etching-growing cycles for the silicon dioxide layer on the surface of the emitter layer during the manufacture of a photosensitive structure, is an effective tool to reduce the recombination losses via the removal of the damaged porous layer and diminish the rate of Auger recombination in the emitter. As a result, the photosensitivity and the efficiency of such structures substantially increase. Furthermore, the indicated additional heat treatment considerably improves the threshold characteristics of the silicon photosensitive structures: their threshold sensitivity increases by more than an order of magnitude after one growing-etching cycle of the oxide layer on the emitter surface and by almost two orders of magnitude after three cycles.

Model representations are proposed for the mechanisms giving rise to the reduction of recombination losses in the emitter layer of photosensitive silicon structures with combined diffusion-field (induced) barriers, if the growing-etching cycles of the silicon dioxide layer on the surface of the emitter layer are applied when manufacturing a photosensitive structure.

1. M.A. Green. The path to 25% silicon solar cell efficiency: history of silicon cell evolution. *Prog. Photovolt: Res. Appl.* **17**, 183 (2009).
2. K. Masuko, M. Shigematsu, T. Hashiguchi, D. Fujishima, M. Kai, N. Yoshimura, T. Yamaguchi, Y. Ichihashi, T. Mishima, N. Matsubara, T. Yamanishi, T. Takahama, M. Taguchi, E. Maruyama, S. Okamoto. Achievement of more than 25% conversion efficiency with crystalline silicon heterojunction solar cells. *IEEE J. Photovolt.* **4**, 1433 (2014).
3. A. Augusto, J. Karas, P. Balaji, S.G. Bowden, R.R. King. Exploring the practical efficiency limit of silicon solar cells using thin solar-grade substrates. *J. Mater. Chem. A* **8**, 16599 (2020).
4. D. Yan, S.P. Phang, Y. Wan, C. Samundsett, D. Macdonald, A. Cuevas. High efficiency n-type silicon solar cells with passivating contacts based on PECVD silicon films doped by phosphorus diffusion. *Solar Energ. Mater. Sol. Cells* **193**, 80 (2019).
5. T.N. Truong, D. Yan, C. Samundsett, R. Basnet, M. Tebyetekerwa, L. Li, F. Kremer, A. Cuevas, D. Macdonald, H.T. Nguyen. Hydrogenation of phosphorus-doped polycrystalline silicon films for passivating contact solar cells. *ACS Appl. Mater. Interf.* **11**, 5554 (2019).
6. W. Chen, J. Stuckelberger, W. Wang, S.P. Phang, D. Kang, C. Samundsett, D. MacDonald, A. Cuevas, L. Zhou, Y. Wan, D. Yan. Influence of PECVD deposition power and pressure on phosphorus-doped polysilicon passivating contacts. *IEEE J. Photovolt.* **10**, 1239 (2020).
7. A. Richter, H. Patel, C. Reichel, J. Benick, S.W. Glunz. Improved silicon surface passivation by ALD Al_2O_3/SiO_2 multilayers with in-situ plasma treatments. *Adv. Mater. Interfaces* **10**, 2202469 (2023).
8. L. Helmich, D.C. Walter, R. Falster, V.V. Voronkov, J. Schmidt. Impact of hydrogen on the boron-oxygen-related lifetime degradation and regeneration kinetics in crystalline silicon. *Sol. Energ. Mater. Sol. Cells* **232**, 111340 (2021).

9. A. Richter, J. Benick, F. Feldmann, A. Fell, M. Hermle, S.W. Glunz. *n*-Type Si solar cells with passivating electron contact: Identifying sources for effciency limitations by wafer thickness and resistivity variation. *Sol. Energ. Mater. Sol. Cells* **173,** 96 (2017).
10. B.E. Deal, M. Sklar, A.S. Grove, E.H. Snow. Characterization of surface state charge of thermally oxidized silicon. *J. Electrochem. Soc.* **114**, 266 (1967).
11. V.G. Litovchenko, A.P. Gorban'. *Fundamentals of Physics of Microelectronic Systems Metal-insulator-semiconductor* (Naukova Dumka, 1978) (in Russian).
12. H. Dib, Z. Benamara, T. Mohammed-Brahim, H. Mazari, N. Bensеddik. Influence of the thermal annealing on the MOS^P structure. *Sensor Lett.* **7**, 765 (2009).
13. K. Kayed, D.B. Kurd. The effect of annealing temperature on the structural and optical properties of Si/SiO_2 composites synthesized by thermal oxidation of silicon wafers. *Silicon* **14**, 5157 (2022).
14. M.A. Green. Photovoltaics: Technology overview. *Energ. Policy* **28**, 989 (2000).
15. V.P. Kostylov. *Photoelectric Energy Conversion Processes in Silicon Multilayer Structures with Diffusion-Field Barriers.* Doctoral dissertation (V. Lashkaryov Institute of Semiconductor Physics, 2009) (in Ukrainian).
16. G.C. Salter, R.E. Thomas. Silicon solar cells using natural inversion layers found in thermally oxidized p-silicon. *Solid State Electron.* **20**, 95 (1977).
17. M.A. Green, F.D. King, J. Shewchun. Minority carrier MIS tunnel diodes and their application to electron-and photovoltaic energy conversion. I. Theory. *Solid-State Electron.* **17**, 551 (1974).
18. Certificate of recognition of measuring capabilities of the Center for testing photo-conversion devices and photovoltaic arrays of the V.E. Lashkaryov Institute of Semiconductor Physics of the National Academy of Sciences of Ukraine, No. PT-448/21, issued on November 09, 2021 by the State Enterprise "All-Ukrainian State Scientific and Production Center for Standardization, Metrology, Certification, and Consumer Rights Protection" of the Ministry of Economy of Ukraine.
19. M.I. Klyui, V.P. Kostylyov, A.V. Makarov, V.V. Chernenko. Metrological aspects of testing photovoltaic solar energy converters. *Sklad. Syst. Protses.* **1**, 42 (2007) (in Ukrainian).
20. A.V. Sachenko, Yu.V. Kryuchenko, V.P. Kostylyov, I.O. Sokolovskyi, A. Abramov, A.V. Bobyl, I.E. Panaiotti, E.I. Terukov. Method for optimizing the parameters of heterojunction photovoltaic cells based on crystalline silicon. *Semiconductors* **50**, 257 (2016).
21. A.V. Sachenko, R.M. Korkishko, V.P. Kostylyov, N.R. Kulish, I.O. Sokolovskyi, A.I. Skrebtii. Simulation of the real efficiencies of high-efficiency silicon solar cells. *Semiconductors* **50**, 523 (2016).
22. A.V. Sachenko, A.I. Shkrebtii, R.M. Korkishko, V.P. Kostylyov, N.R. Kulish, I.O. Sokolovskyi. Features of photoconversion in highly efficient silicon solar cells. *Semiconductors* **49**, 264 (2015).
23. T. Trupke, M.A. Green, P. Würfel, P.P. Altermatt, A. Wang, J. Zhao, R. Corkish. Temperature dependence of the radiative recombination coefficient of intrinsic crystalline silicon. *J. Appl. Phys.* **94**, 4930 (2003).
24. A.P. Gorban', V.A. Zuev, V.P. Kostylyov, A.V. Sachenko, A.A. Serba, V.V. Chernenko. About the temperature dependences of the equilibrium and non-equilibrium parameters in silicon. *Optoelektron. Poluprov. Tekhn.* **36**, 161 (2001) (in Russian).
25. A.V. Sachenko, V.P. Kostylyov, V.M. Vlasiuk, I.O. Sokolovskyi, M.A. Evstigneev, T.V. Slusar, V.V. Chernenko. Modeling of characteristics of highly efficient textured solar cells based on c-silicon. The influence of recombination in the space charge region. *Semicond. Phys. Quant. Electron. Optoelectron.* **26**, 005 (2023).
26. A.V. Sachenko, V.P. Kostylyov, V.M. Vlasiuk, I.O. Sokolovskyi, M. Evstigneev, D.F. Dvernikov, R.M. Korkishko, V.V. Chernenko. Space charge region recombination, nonradiative exciton recombination and the band-narrowing effect in high-efficiency silicon solar cells. *Semicond. Phys. Quant. Electron. Optoelectron.* **26**, 127 (2023).
27. K.D. Glinchuk, N.M. Litovchenko, Z.A. Salnik, S.I. Skryl. Effect of heat treatment on the minority carrier lifetime in oxygen-containing silicon. *Phys. Status Solidi A* **79**, 159 (1983).
28. A.P. Gorban', V.P. Kostylyov, V.V. Chernenko. Genesis of generational and charge characteristics of the $Si-SiO_2$ system during the manufacture of KMOS GIS. *Optoelektron. Poluprov. Tekhn.* **24**, 61 (1992) (in Russian).
29. D.A. Clugston, P.A. Basore. PC1D Version 5: 32-bit solar cell simulation on personal computers. In: *Proceedings of the 26th IEEE Photovoltaic Specialists Conference (PVSC 1997), September 1997, Anaheim, CA, USA* (IEEE, 1997), p. 207.
30. A.P. Gorban', V.P. Kostylyov, V.G. Litovchenko, I.B. Nikolin, A.A. Serba. The "self-gettering" effect at the formation of diffusion *p-n*-junctions in silicon. *Mikroelektronika* **22**, 22 (1993) (in Russian).
31. A. Cuevas, D. MacDonald, M. Kerr, C. Samundsett, A. Sloan, S. Shea, A. Leo, M. Mrcarica, S. Winderbaum. Evidence of impurity gettering by industrial phosphorus diffusion. In: *Proceedings of the 28 IEEE Photovoltaic Specialists Conference (PVSC 2000), Anchorage, Alaska, USA, September 15–22, 2000* (IEEE, 2000), p. 244.
32. R.L. Meek, T.E. Seidel. Enhanced solubility and ion pairing of Cu and Au in heavily doped silicon at high temperatures. *J. Phys. Chem. Solids* **36**, 731 (1975).
33. L. Baldi, G. Cerofolini, G. Ferla. Heavy-metal gettering in silicon-device processing. *J. Electrochem. Soc.* **127**, 164 (1980).

Received 01.08.23.

Translated from Ukrainian by O.I. Voitenko

В.П. Костильов, А.В. Саченко,
Т.В. Слусар, В.В. Черненко

ЗМЕНШЕННЯ РЕКОМБІНАЦІЙНИХ ВТРАТ У ДИФУЗІЙНИХ ПРИПОВЕРХНЕВИХ ЕМІТЕРНИХ ШАРАХ ФОТОЧУТЛИВИХ КРЕМНІЄВИХ СТРУКТУР n^+-p-p^+

Встановлено, що після проведення операції дифузії при створенні n^+-емітера фоточутливих структур типу n^+-p-p^+ його приповерхневий шар має значні структурні пошкодження з підвищеними рекомбінаційними втратами. Проведено дослідження впливу додаткових обробок у вигляді циклів стравлювання-вирощування шару двоокису кремнію на поверхні емітера при виготовленні таких фоточутливих кремнієвих структур на їхні фотоелектричні і рекомбінаційні характеристики. Показано, що застосування таких додаткових обробок у процесі виготовлення фоточутливих кремнієвих структур дозволяє ефективно зменшити рекомбінаційні втрати і, тим самим, значно покращити фотоелектричні параметри таких структур, в тому числі і їхню спектральну та порогову фоточутливість.

Ключові слова: фоточутлива кремнієва структура, приповерхневий шар, емітер, рекомбінаційні втрати, термообробки, шар двоокису кремнію.